Experimental demonstration of five-photon entanglement and open-destination teleportation

Zhi Zhao[1], Yu-Ao Chen[1], An-Ning Zhang[1], Tao Yang[1], Hans J. Briegel[2] & Jian-Wei Pan[1,3]

[1]*Department of Modern Physics and Hefei National Laboratory for Physical Sciences at Microscale, University of Science and Technology of China, Hefei, Anhui, 230026, China*
[2]*Institute for Theoretical Physics, University of Innsbruck, and Institute for Quantum Optics and Quantum Information, Austrian Academy of Sciences, A-6020 Innsbruck, Austria*
[3]*Physikalisches Institut, Universität Heidelberg, Philosophenweg 12, D-69120 Heidelberg, Germany*

Quantum-mechanical entanglement of three[1,2] or four[3,4] particles has been achieved experimentally, and has been used to demonstrate the extreme contradiction between quantum mechanics and local realism[5,6]. However, the realization of five-particle entanglement remains an experimental challenge. The ability to manipulate the entanglement of five or more particles is required[7,8] for universal quantum error correction. Another key process in distributed quantum information processing[9,10], similar to encoding and decoding, is a teleportation protocol[11,12] that we term 'open-destination' teleportation. An unknown quantum state of a single particle is teleported onto a superposition of N particles; at a later stage, this teleported state can be read out (for further applications) at any of the N particles, by a projection measurement on the remaining particles. Here we report a proof-of-principle demonstration of five-photon entanglement and open-destination teleportation (for $N = 3$). In the experiment, we use two entangled photon pairs to generate a four-photon entangled state, which is then combined with a single-photon state. Our experimental methods can be used for investigations of measurement-based quantum computation[9,10] and multi-party quantum communication[13,14].

In our experiment, the way to entangle five photons is a straightforward generalization of the schemes suggested for observation of three- and four-photon Greenberger–Horne–Zeilinger (GHZ) entanglement[15,16]. We start from two polarization-entangled photon pairs, 2-3 and 4-5, which are in the state $|\Phi^+\rangle$ (Fig. 1a). We use the usual Bell states

$$|\Phi^{\pm}\rangle_{ij} = \tfrac{1}{\sqrt{2}}(|H\rangle_i|H\rangle_j \pm |V\rangle_i|V\rangle_j)$$
$$|\Psi^{\pm}\rangle_{ij} = \tfrac{1}{\sqrt{2}}(|H\rangle_i|V\rangle_j \pm |V\rangle_i|H\rangle_j) \quad (1)$$

where H and V denote respectively horizontal and vertical linear polarizations, and i and j index the spatial modes of the photons. One photon out of each pair (3 and 4) is then steered to a polarizing beam splitter (PBS) where the path lengths of each photon have been adjusted such that they arrive simultaneously. Because the PBS transmits H and reflects V polarization, coincidence detection between the two outputs of PBS_{34} implies that either both photons 3 and 4 are H-polarized or both are V-polarized, and thus projects the four-photon state onto a two-dimensional subspace spanned by $|H\rangle_2|H\rangle_3|H\rangle_4|H\rangle_5$ and $|V\rangle_2|V\rangle_3|V\rangle_4|V\rangle_5$. After PBS_{34}, the renormalized state corresponding to a fourfold coincidence (before photon 2 passes through PBS_{12}) is

$$|\Phi\rangle_{2345} = \frac{1}{\sqrt{2}}(|H\rangle_2|H\rangle_3|H\rangle_4|H\rangle_5 + |V\rangle_2|V\rangle_3|V\rangle_4|V\rangle_5) \quad (2)$$

which exhibits four-photon GHZ entanglement[4,15].

To generate five-photon GHZ entanglement, we further prepare photon 1 in the state $\frac{1}{\sqrt{2}}(|H\rangle_1 + |V\rangle_1$ and adjust the path lengths of photons 1 and 2 such that they also arrive at PBS_{12} simultaneously. Then, we see that after the photons pass through the two PBS, the state corresponding to a fivefold coincidence is given by:

$$|\Phi\rangle_{12345} = \frac{1}{\sqrt{2}}(|H\rangle_1|H\rangle_2|H\rangle_3|H\rangle_4|H\rangle_5 + |V\rangle_1|V\rangle_2|V\rangle_3|V\rangle_4|V\rangle_5) \quad (3)$$

This is exactly a five-photon GHZ state.

The scheme described above deserves some further comments. First, the five-photon entanglement here is observed only under the condition that there is one and only one photon in each of the five output modes. This post-selective feature, however, does not prevent us from performing an experimental test of quantum nonlocality[5,6] or in-principle verification of elements of linear optical quantum information processing[17,18].

Moreover, the set-up sketched in Fig. 1a can also be used to realize open-destination teleportation, which can be viewed as encoding followed by decoding. In the open-destination teleportation scheme, we use the four-particle GHZ state (equation (2)) as the resource and photon 1 as the 'teleportee'. To see this, we consider a specific example (Fig. 1b). Suppose that photon 1 is in a general unknown polarization state $|\Psi\rangle_1 = \alpha|H\rangle_1 + \beta|V\rangle_1$. In order to overcome the unavoidable decoherence effect on the state $|\Psi\rangle_1$, one could exploit quantum error correction. For example, to detect and correct the bit-flip error[8,19], we could encode the unknown state of photon 1 into a three-qubit superposition, say $|\Psi\rangle_{345} = \alpha|H\rangle_3|H\rangle_4|H\rangle_5 + \beta|V\rangle_3|V\rangle_4|V\rangle_5$. Note that, to realize universal

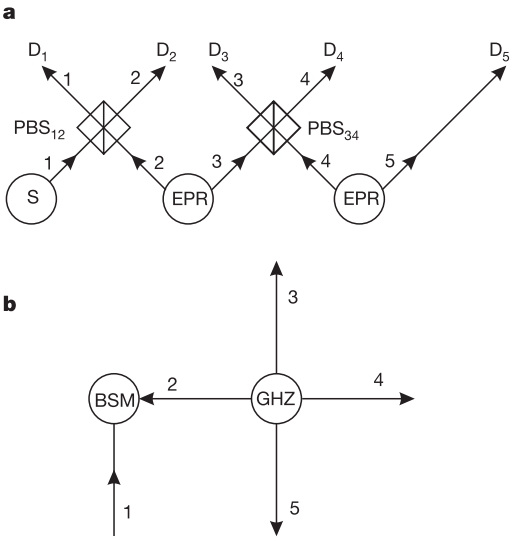

Figure 1 Diagrams showing the principles of generating five-photon entanglement and of achieving open-destination teleportation. **a**, Two Einstein-Podolsky-Rosen (EPR) entangled photon sources each emit one polarization-entangled photon pair, which is in the state $|\Phi^+\rangle = 1/\sqrt{2}(|H\rangle|H\rangle + |V\rangle|V\rangle)$. The single-photon source (S) emits a single photon state $\frac{1}{\sqrt{2}}(|H\rangle_1 + |V\rangle_1)$. After the photons 1, 2, 3 and 4 pass through the two polarizing beam splitters PBS_{12} and PBS_{34}, conditional on detecting one photon in each of the five output modes, the five photons will exhibit five-photon Greenberger-Horne-Zeilinger (GHZ) entanglement. **b**, The GHZ entanglement source emits a four-photon maximally entangled state $|\Phi\rangle_{2345} = \frac{1}{\sqrt{2}}(|H\rangle_2|H\rangle_3|H\rangle_4|H\rangle_5 + |V\rangle_2|V\rangle_3|V\rangle_4|V\rangle_5)$. Photon 1 is in a general unknown polarization state $|\Psi\rangle_1 = \alpha|H\rangle_1 + \beta|V\rangle_1$. By performing a joint Bell-state measurement (BSM) between photons 1 and 2, we can follow the teleportation protocol to transfer the initial state of photon 1 to a multi-particle superposition $|\Psi\rangle_{345} = \alpha|H\rangle_3|H\rangle_4|H\rangle_5 + \beta|V\rangle_3|V\rangle_4|V\rangle_5$. Moreover, by further performing a polarization analysis on any two of the three photons 3, 4 and 5 in the $+/-$ basis one can convert the remaining photon into the initial state of photon 1.

quantum error correction, a more complicated encoding procedure is needed.

To achieve the three-qubit encoding, we first prepare photons 2, 3, 4 and 5 in the four-photon GHZ state $|\Phi\rangle_{2345}$ of equation (2). Then, using the four Bell states of photons 1 and 2 the overall state of the five photons can be rewritten as:

$$\begin{aligned}|\Psi\rangle_{12345} &= |\Psi\rangle_1|\Phi\rangle_{2345} \\ &= \frac{1}{2}[|\Phi^+\rangle_{12}(\alpha|H\rangle_3|H\rangle_4|H\rangle_5 + \beta|V\rangle_3|V\rangle_4|V\rangle_5) \\ &\quad + |\Phi^-\rangle_{12}(\alpha|H\rangle_3|H\rangle_4|H\rangle_5 - \beta|V\rangle_3|V\rangle_4|V\rangle_5) \\ &\quad + |\Psi^+\rangle_{12}(\alpha|V\rangle_3|V\rangle_4|V\rangle_5 + \beta|H\rangle_3|H\rangle_4|H\rangle_5) \\ &\quad + |\Psi^-\rangle_{12}(\alpha|V\rangle_3|V\rangle_4|V\rangle_5 - \beta|H\rangle_3|H\rangle_4|H\rangle_5)]\end{aligned} \quad (4)$$

This implies that a joint Bell measurement on photons 1 and 2 would thus project the state of photons 3, 4 and 5 into one of the four corresponding states, as shown in equation (4). Depending on the measurement results on photons 1 and 2, one can then perform a local unitary transformation, independent of $|\Psi\rangle_1$, on photons 3, 4 and 5 to convert the state into a three-particle superposition of $|\Psi\rangle_{345}$. This is how encoding works. During the encoding operation, the unknown state of a single particle is teleported onto a three-particle superposition, and can thus be protected against bit-flip error[8,19].

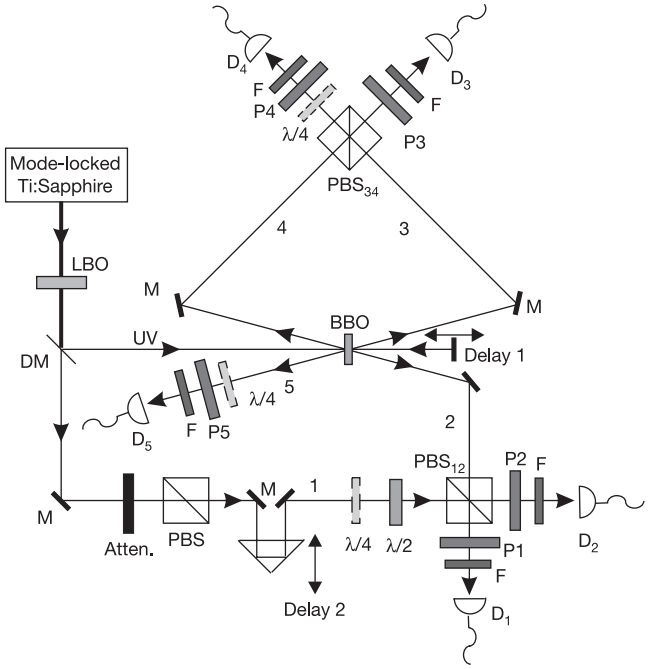

Figure 2 Set-up for experimental demonstration of five-photon entanglement and open-destination teleportation. To prepare the desired stable high-intensity source of entangled photons, various methods have been used. First, we properly focus the infrared pulse on the LBO crystal to achieve the best up-conversion efficiency. Meanwhile, to avoid damage to the LBO crystal caused by the focusing laser beam, we assemble the LBO crystal in a closed but transparent tube of oxygen. Second, by using a compact set-up and by focusing the UV pump onto the BBO crystal, we achieve both better collection efficiency and production rate of entangled photon pairs. Third, two CCD cameras (not shown) are used to monitor the laser beam direction. Thus, with the help of a feedback loop we can well stabilize the beam direction. In this way, we managed to obtain an average UV pump power of 480 mW and observe an average twofold coincidence of $2.4 \times 10^4\,s^{-1}$ both in modes 2–3 and 4–5. The mirrors Delay 1 and Delay 2 are used to adjust the time delay of photons 3 and 4 and of photons 1 and 2, respectively. In order to interfere photons 1 and 2 at PBS_{12} and photons 3 and 4 at PBS_{34}, narrow band-width filters F ($\Delta\lambda_{FWHM} = 3$ nm) and fibre-coupled detectors D1, …, D5 have been used to ensure good temporal and spatial overlap of photons 1 and 2 and of photons 3 and 4. The wave plates $\lambda/2$ and $\lambda/4$ in front of PBS_{12} are used to transform the horizontal polarization into linear $+/-$ or circular *R*/*L* polarization. The polarizers P1,…, P5 oriented at $+/-$ basis and the $\lambda/4$ plate in front of the detectors allow measurement of linear $+/-$ or circular *R*/*L* polarization.

To demonstrate the working principle of the encoding operation, it is sufficient to identify one of the four Bell states (say, $|\Phi^+\rangle_{12}$) although this results in a reduced efficiency—the fraction of success—of 25%. The encoding operation can be achieved using the set-up shown in Fig. 1a. First, the set-up provides the necessary four-photon GHZ entanglement $|\Phi\rangle_{2345}$ after photons 3 and 4 passes through PBS_{34}. Second, as demonstrated in a recent experiment[4], the projection onto state $|\Phi^+\rangle_{12}$ can be accomplished by performing a joint polarization measurement in the $+/-$ basis behind PBS_{12}, where $|\pm\rangle = \frac{1}{\sqrt{2}}(|H\rangle \pm |V\rangle)$. As stated in ref. 6, registering a $|+\rangle_1|+\rangle_2$ or $|-\rangle_1|-\rangle_2$ coincidence acts as a projection onto $|\Phi^+\rangle_{12}$. This projection leaves photons 3, 4 and 5 in the state: $|\Psi\rangle_{345} = \alpha|H\rangle_3|H\rangle_4|H\rangle_5 + \beta|V\rangle_3|V\rangle_4|V\rangle_5$.

At a later stage, we can then use the decoding operation to read out or apply desired specific operations on the unknown state for further quantum information processing. To do so, we perform a local polarization measurement on two of the three photons 3, 4 and 5 in the $+/-$ basis. For example, if we perform a $\pm$ polarization analysis on photons 4 and 5, and if the measurement results on these two photons are the same — that is, $|+\rangle_4|+\rangle_5$ or $|-\rangle_4|-\rangle_5$—then photon 3 is left in the state $|\Psi\rangle_3 = \alpha|H\rangle_3 + \beta|V\rangle_3$. If the results are opposite, namely $|+\rangle_4|-\rangle_5$ or $|-\rangle_4|+\rangle_5$, then photon 3 is left in the state $\alpha|H\rangle_3 - \beta|V\rangle_3$. In the second case, one can simply perform a local phase flip operation on photon 3 to convert its state into $|\Psi\rangle_3$, that is, the original state of photon 1. We can thus teleport the unknown quantum state from photon 1 to photon 3.

We note that, in a similar manner, the initial state of photon 1 can also be teleported either onto photon 4 or photon 5 by performing a polarization measurement either on photons 3 and 5 or on photons 3 and 4 in the $+/-$ basis. In contrast to the original teleportation scheme[11], after the encoding operation the destination of teleportation is left open until we perform a polarization measurement on two of the remaining three photons. This implies that, even though photons 3, 4 and 5 are far apart, one can still choose which particle should act as the output—that is, the particle to which the initial state of photon 1 is transferred[12]. This is why we have called such an encoding–decoding procedure 'open-destination' teleportation. It is therefore a generalization of standard teleportation, in which no prior agreement on the final destination of the teleportation is necessary. Open-destination teleportation is possible if the parties initially share a multi-party entangled state, such as the GHZ state, but more generally any graph state[20] (of which the cluster state[21] is another example) can be used. Graph states are natural generalizations of the Einstein-Podolsky-Rosen (EPR) state, which plays a key role in novel schemes of quantum information processing[21]. A potential application of the open-destination teleportation is the scheme of quantum computation introduced by Gottesman and Chuang[9], using GHZ states and teleportation as a resource to realize quantum gates. Similarly, the ability to establish flexible teleportation channels with an entangled (cluster) state is a central ingredient in the one-way quantum computer[10].

Although our scheme to manipulate five-photon entanglement is theoretically simple, its experimental realization is very challenging. So far, spontaneous parametric down-conversion (SPDC) is still the best source of entangled photons, which is therefore used as the basic entanglement resource in the present experiment. However, owing to the probabilistic feature of SPDC, the coincidence count rate in our five-photon experiment would be very low. To overcome

this difficulty, we combine a high-intensity source of entangled photons and a source of pseudo-single photons so that we can collect enough experimental data to confirm the existence of five-photon entanglement within a reasonable time.

A schematic drawing of our experimental set-up is shown in Fig. 2. In the experiment, a light pulse from a mode-locked Ti:sapphire laser (with a duration of 200 fs, a repetition rate of 76 MHz and a central wavelength of 788 nm) first passes through a frequency doubler, that is, the LBO crystal (LiB_3O_5). Behind the LBO, three dichroic beamsplitters (DM) are used to separate the mixed ultraviolet (UV) and infrared light components. The UV pulse further passes through a β-barium borate (BBO) crystal twice to generate two entangled photon pairs in the input modes 2–3 and 4–5[22], where both pairs are in the desired Bell state, $|\Phi^+\rangle$. The

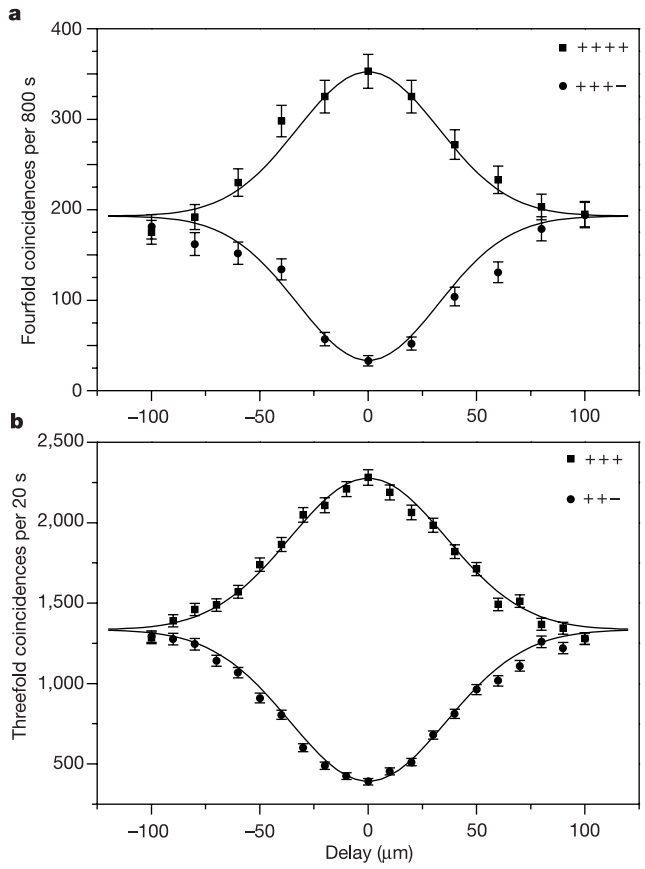

Figure 3 Experimental results showing the procedure used to achieve perfect temporal overlap for photons 1 and 2 and for photons 3 and 4. **a**, The two fourfold coincidence curves were obtained for the polarization settings of $|+\rangle_2|+\rangle_3|+\rangle_4|+\rangle_5$ and $|+\rangle_2|+\rangle_3|+\rangle_4|-\rangle_5$ as a function of the position of the Delay 1 mirror. During the measurement, PBS_{34} was inserted into the crossing position of modes 3 and 4 while PBS_{12} was lowered out of the crossing position of modes 1 and 2. Photon 2 was registered by D1. By fixing the Delay 1 mirror to the position where we observe the best four-photon interference visibility (that is, the centre of the peak and dip) we can achieve perfect temporal overlap for photons 3 and 4. Thus, the fourfold coincidence among the detectors D1, D3, D4 and D5 corresponds to the four-photon GHZ state of equation (2)[15]. The coherent superposition between the terms $|H\rangle_2|H\rangle_3|H\rangle_4|H\rangle_5$ and $|V\rangle_2|V\rangle_3|V\rangle_4|V\rangle_5$ was confirmed with an excellent interference visibility of 82%. **b**, The two threefold coincidence curves were obtained for the polarization settings of $|+\rangle_1|+\rangle_2|+\rangle_3$ and $|+\rangle_1|+\rangle_2|-\rangle_3$ as a function of the Delay 2 position. Here, PBS_{12} was inserted into the crossing position of modes 1 and 2 while PBS_{34} was lowered out of the crossing position of modes 3 and 4. Photon 3 was registered by D4. Similarly, by setting the Delay 2 position to the centre of the peak and dip of the threefold coincidence, we can achieve perfect temporal overlap for photons 1 and 2. At zero delay, the threefold coincidence among the detectors D1, D2 and D4 is a post-selective three-photon GHZ entanglement[16]. In our three-photon entanglement, the visibility was observed to be 68%. After achieving the perfect time overlap between photons 1 and 2, PBS_{34} was raised back to its original position to implement five-photon entanglement. The error bars here and in Fig. 4 are defined as the square root of the observed multi-fold coincidence.

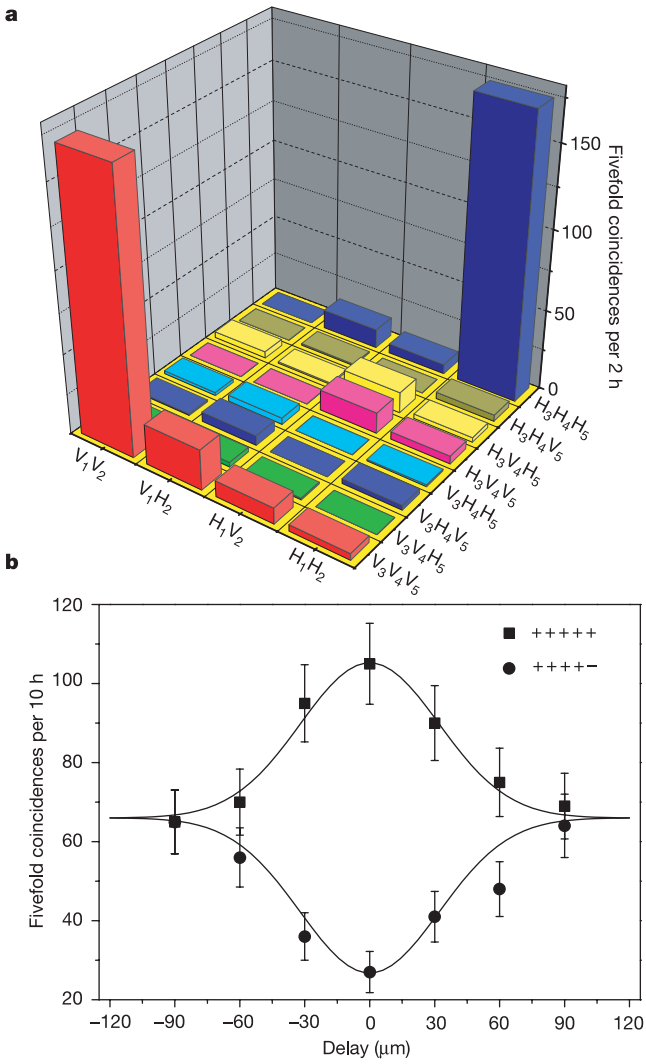

Figure 4 Experimental results for the observation of five-photon entanglement. **a**, To verify that five-photon GHZ entanglement has been successfully generated, we first measure the 32 possible components in the *H*/*V* basis. The measurement results show that the signal-to-noise ratio, that is, the ratio of any of the desired components to any of the 30 other non-desired ones, is about 40:1 on average. This confirms that within the experimental precision only the desired *HHHHH* and *VVVVV* terms are present. **b**, To further demonstrate that these two terms are indeed in a coherent superposition, we also perform a joint polarization measurement on all five photons in the + /− basis. The two curves were obtained for the polarization settings of $|+\rangle_1|+\rangle_2|+\rangle_3|+\rangle_4|+\rangle_5$ and $|+\rangle_1|+\rangle_2|+\rangle_3|+\rangle_4|-\rangle_5$ as a function of the position of the Delay 1 mirror with the position of the Delay 2 mirror fixed, which confirms the coherent superposition of the *HHHHH* and *VVVVV* terms with a visibility of 59%. In the experiment, the non-desired components are mainly due to the limited quality of the polarization optics and the double emissions in the source of single and entangled photons. The double emissions contribute around 3% to overall fivefold events. Without additional assumptions, it is not possible to use the above data to give an explicit estimation of the fidelity of our five-photon entanglement. However, if we are allowed to assume that the non-desired components in the *H*/*V* basis contribute equally to the $|+\rangle_1|+\rangle_2|+\rangle_3|+\rangle_4|+\rangle_5$ and $|+\rangle_1|+\rangle_2|+\rangle_3|+\rangle_4|-\rangle_5$ terms, the fidelity for our five-photon source to be in the state $|\Phi\rangle_{12345}$ is estimated to be 68%. Assuming that the non-desired components only contribute to the $|+\rangle_1|+\rangle_2|+\rangle_3|+\rangle_4|-\rangle_5$ term, a lower bound of the fidelity is estimated to be 55%.

transmitted near-infrared pulse is attenuated by combining a beam attenuator ('Atten.' in Fig. 2) and a polarizing beam splitter (PBS) to a weak coherent state such that there is only a very small probability of containing a single photon for each pulse ($\sim$0.05 in our experiment). We can thus prepare the required single photon state[16]. Note that such a pseudo-single photon source has been used in numerous experiments[23,24]. Throughout the experiment, the coincidence time-window is set to be 4 ns, which ensures that accidental coincidence is negligible.

In order to prepare a stable high-intensity source of entangled photons, various efforts have been made (see Fig. 2 legend). Compared to the source of entangled photons developed in the recent experiments[25], our source is not only brighter, but, most significantly, it is also ultra-stable—it can be easily stabilized for a couple of days.

Implementation of five-photon entanglement requires that photons 1 and 2 (3 and 4) have good spatial and temporal overlap at PBS_{12} (PBS_{34}). To achieve this, the two outputs of PBS_{12} and PBS_{34} are spectrally filtered ($\Delta\lambda_{FWHM} = 3$ nm) and monitored by fibre-coupled single-photon detectors[26]. Moreover, perfect temporal overlap is accomplished by observing interference fringes of three- and four-photon entanglement in the $+/-$ basis (see Fig. 3 legend). The experimental three- and four-photon interference visibilities were observed to be 68% and 82%, respectively. Remarkably, the observed coincidence rate of our three-photon entanglement source is about 500 s^{-1}, which is three orders of magnitude higher than in a recent experiment[27]. After achieving perfect time overlap between photons 1 and 2 and between photons 3 and 4, according to equation (3) the fivefold coincidence among the detectors D1, D2, D3, D4 and D5 will then exhibit five-photon GHZ entanglement.

To verify experimentally that five-photon entanglement has been successfully obtained, we first show that under the condition of registering a fivefold coincidence only the $|H\rangle|H\rangle|H\rangle|H\rangle|H\rangle$ and $|V\rangle|V\rangle|V\rangle|V\rangle|V\rangle$ components are observed, but no others. This was done by comparing the counts of all 32 possible polarization combinations, $|H\rangle|H\rangle|H\rangle|H\rangle|H\rangle$, …, $|V\rangle|V\rangle|V\rangle|V\rangle|V\rangle$. The measurement results (Fig. 4a) in the H/V basis show that the signal-to-noise ratio, defined as the ratio of any of the desired components to any of the 30 other non-desired ones, is about 40:1 on average.

Second, we further perform a polarization measurement in the $+/-$ basis to verify that the two terms of $|H\rangle|H\rangle|H\rangle|H\rangle|H\rangle$ and $|V\rangle|V\rangle|V\rangle|V\rangle|V\rangle$ are indeed in a coherent superposition. Transforming $|\Phi\rangle_{12345}$ to the $+/-$ linear polarization basis yields an expression containing 16 (out of 32 possible) terms, each with an odd number of $|+\rangle$ components. Combinations with even numbers of $|+\rangle$ components do not occur. As a test for coherence we can check the presence or absence of various components. In Fig. 4b we compare the $|+\rangle|+\rangle|+\rangle|+\rangle|+\rangle$ and $|+\rangle|+\rangle|+\rangle|+\rangle|-\rangle$ count rates as a function of the Delay 1 mirror position (see Fig. 2) while the Delay 2 is at zero delay. When the Delay 1 is also at zero delay, the unwanted terms were found to be suppressed with an average visibility of 0.59 $\pm$ 0.07, which is sufficient to violate a five-particle Bell-type inequality imposed by local realism[28]. Therefore, the measurement results in Fig. 4 clearly demonstrate the existence of five-particle entanglement.

We now show how the same set-up can be used to implement open-destination teleportation. To demonstrate that our open-destination teleportation protocol works for a general unknown polarization state of photon 1, we choose to teleport $|+\rangle$ and $|-\rangle$ linear polarization states $\frac{1}{\sqrt{2}}(|H\rangle \pm |V\rangle)$ and right-hand ($|R\rangle$) and left-hand ($|L\rangle$) circular polarization states $\frac{1}{\sqrt{2}}(|H\rangle \pm i|V\rangle)$. In the experiment, we decided to analyse the Bell state $|\Phi^+\rangle_{12}$. The required projection onto $|\Phi^+\rangle_{12}$ was achieved by registering a $|+\rangle_1|+\rangle_2$ coincidence behind PBS_{12}. Then, as already discussed, conditional on a $|+\rangle|+\rangle$ coincidence detection in the output modes 3 and 4, photon 5 will be left in the initial state of photon 1, that is, the unknown state of photon 1 is teleported to photon 5. In order to demonstrate that the initial state of photon 1 can also be teleported to some other location (for example, location 4 of Fig. 1b), we can, in a similar manner, perform a polarization analysis on photons 3 and 5 in the $+/-$ linear polarization basis. Then, conditional on a $|+\rangle|+\rangle$ coincidence detection in the output modes 3 and 5, photon 4 will be left in the initial state of photon 1.

In our experiment, the integration time for each teleportation measurement is about 10 hours. As shown in Fig. 4b, in every polarization analysis measurement the fivefold coincidence rate is about 100 for the maximum (desired) component and 20 for the minimum (non-desired) component per 10 hours. The experimental fidelities of teleportation from photon 1 to photon 5 and from photon 1 to photon 4 for $+/-$ linear and R/L circular polarization states are shown in Table 1. From Table 1, one can see that all the observed teleportation fidelities ($\sim$0.80 $\pm$ 0.04) are well above the classical limit of two-thirds, hence fully demonstrating open-destination teleportation.

Although compared to the previous experiments[1,4,29] our experimental demonstration of five-photon entanglement and open-destination teleportation might seem to be only a modest step forward, the implications are profound. First, our experiment has demonstrated the ability to manipulate five-particle entanglement, which is the threshold number of qubits required for universal error correction[7,8]. Second, the realization of open-destination teleportation opens up new possibilities for distributed quantum information processing[9,10]. Last, the techniques developed in the present experiment enable experimental investigations of a number of quantum protocols. Whereas our high-intensity three-photon entanglement source immediately allows an experimental realization of quantum secret sharing[13,14], the five-photon experimental set-up that we report here should also allow experimental demonstrations of both bit-flip error rejection for quantum communication[19] and a non-destructive CNOT gate for quantum computation[30]. □

Table 1 **Fidelities of open-destination teleportation at two different locations**

Polarization	Fidelities	
	Location 4	Location 5
$\|+\rangle$	0.79 ± 0.04	0.80 ± 0.03
$\|-\rangle$	0.81 ± 0.04	0.77 ± 0.04
$\|R\rangle$	0.75 ± 0.04	0.79 ± 0.04
$\|L\rangle$	0.79 ± 0.04	0.82 ± 0.03

Received 12 February; accepted 10 May 2004; doi:10.1038/nature02643.

1. Bouwmeester, D., Pan, J.-W., Daniell, M., Weinfurter, H. & Zeilinger, A. Observation of three-photon Greenberger-Horne-Zeilinger entanglement. *Phys. Rev. Lett.* **82,** 1345–1349 (1999).
2. Rauschenbeutel, A. *et al.* Step-by-step engineered multiparticle entanglement. *Science* **288,** 2024–2028 (2000).
3. Sackett, C. A. *et al.* Experimental entanglement of four particles. *Nature* **404,** 256–259 (2000).
4. Pan, J.-W., Daniell, M., Gasparoni, S., Weihs, G. & Zeilinger, A. Experimental demonstration of four-photon entanglement and high-fidelity teleportation. *Phys. Rev. Lett.* **86,** 4435–4439 (2001).
5. Pan, J.-W., Bouwmeester, D., Daniell, M., Weinfurter, H. & Zeilinger, A. Experimental test of quantum non-locality in three-photon Greenberger-Horne-Zeilinger entanglement. *Nature* **403,** 515–519 (2000).
6. Zhao, Z. *et al.* Experimental violation of local realism by four-photon Greenberger-Horne-Zeilinger entanglement. *Phys. Rev. Lett.* **91,** 180401 (2003).
7. Bennett, C. H., DiVincenzo, D. P., Smolin, J. A. & Wootters, W. K. Mixed-state entanglement and quantum error correction. *Phys. Rev. A.* **54,** 3824–3851 (1996).
8. Laflamme, R., Miquel, C., Paz, J. P. & Zurek, W. H. Perfect quantum error correcting code. *Phys. Rev. Lett.* **77,** 198–201 (1996).
9. Gottesman, D. & Chuang, I. L. Demonstrating the viability of universal quantum computation using teleportation and single-qubit operations. *Nature* **402,** 390–393 (1999).
10. Raussendorf, R. & Briegel, H. J. A one-way quantum computer. *Phys. Rev. Lett.* **86,** 5188–5191 (2001).
11. Bennett, C. H. *et al.* Teleporting an unknown quantum state via dual classical and Einstein-Podolsky-Rosen channels. *Phys. Rev. Lett.* **83,** 3081–3084 (1993).
12. Karlsson, A. & Bourennane, M. Quantum teleportation using three-photon entanglement. *Phys. Rev. A* **58,** 4394–4400 (1998).
13. Hillery, M., Buzek, V. & Berthiaume, A. Quantum secret sharing. *Phys. Rev. A.* **59,** 1829–1834 (1999).
14. Scarani, V. & Gisin, N. Quantum communication between N partners and Bell's inequalities. *Phys. Rev. Lett.* **87,** 117901 (2001).

15. Zeilinger, A., Horne, M. A., Weinfurter, H. & Zukowski, M. Three-particle entanglements from two entangled pairs. *Phys. Rev. Lett.* **78,** 3031–3034 (1997).
16. Rarity, J. G. & Tapster, P. R. Three-particle entanglement from entangled photon pairs and a weak coherent state. *Phys. Rev. A* **59,** R35–R38 (1999).
17. Pan, J.-W., Simon, C., Brukner, C. & Zeilinger, A. Entanglement purification for quantum communication. *Nature* **410,** 1067–1070 (2001).
18. Knill, E., Laflamme, R. & Milburn, G. J. A scheme for efficient quantum computation with linear optics. *Nature* **409,** 46–52 (2001).
19. Bouwmeester, D. Bit-flip-error rejection in optical quantum communication. *Phys. Rev. A* **63,** R040301 (2001).
20. Hein, M., Eisert, J., & Briegel, H.J. Multi-party entanglement in graph states. *Phys. Rev. A* **69,** 06231 (2004).
21. Briegel, H. J & Raussendorf, R. Persistent entanglement in arrays of interacting particles. *Phys. Rev. Lett.* **86,** 910–913 (2001).
22. Kwiat, P. G. *et al.* New high intensity source of polarization-entangled photon pairs. *Phys. Rev. Lett.* **75,** 4337–4341 (1995).
23. Kurtsiefer, C. *et al.* A step towards global key distribution. *Nature* **419,** 450 (2002).
24. De Martini, F., Buzek, V., Sciarrino, F. & Sias, C. Experimental realization of the quantum universal NOT gate. *Nature* **419,** 815–818 (2002).
25. Pan, J.-W., Gasparoni, S., Rupert, U., Weihs, G. & Zeilinger, A. Experimental entanglement purification of arbitrary unknown states. *Nature* **423,** 417–422 (2003).
26. Zukowski, M., Zeilinger, A. & Weinfurter, H. Entangling photons radiated by independent pulsed source. *Ann. NY Acad. Sci.* **755,** 91–102 (1995).
27. Pittman, T. B., Jacobs, B. C. & Franson, J. D. Probabilistic quantum encoder for single-photon qubits. *Phys. Rev. A* **69,** 042306 (2004).
28. Zukowski, M. & Kaszlikowski, D. Critical visibility for N-particle Greenberger-Horne-Zeilinger correlations to violate local realism. *Phys. Rev. A* **56,** R1682–R1685 (1997).
29. Bouwmeester, D. *et al.* Experimental quantum teleportation. *Nature* **390,** 575–579 (1997).
30. Pittman, T. B., Jacobs, B. C. & Franson, J. D. Demonstration of nondeterministic quantum logic operations using linear optical elements. *Phys. Rev. Lett.* **88,** 257902 (2002).

Acknowledgements This work was supported by the National Natural Science Foundation of China, the Chinese Academy of Sciences, the National Fundamental Research Program and the German Research Foundation (DFG).

Competing interests statement The authors declare that they have no competing financial interests.

Correspondence and requests for materials should be addressed to J.-W.P. (jian-wei.pan@physi.uni-heidelberg.de).

Cyclotron frequency shifts arising from polarization forces

James K. Thompson, Simon Rainville & David E. Pritchard

Research Laboratory of Electronics, MIT-Harvard Center for Ultracold Atoms, and Department of Physics, Massachusetts Institute of Technology, 77 Massachusetts Avenue, Cambridge, Massachusetts 02139, USA

The cyclotron frequency of a charged particle in a uniform magnetic field B is related to its mass m and charge q by the relationship $\omega_c = qB/m$. This simple relationship forms the basis for sensitive mass comparisons using ion cyclotron resonance mass spectroscopy, with applications ranging from the identification of biomolecules[1] and the study of chemical reaction rates[2] to determinations of the fine structure constant of atomic spectra[3]. Here we report the observation of a deviation from the cyclotron frequency relationship for polarizable particles: in high-accuracy measurements of a single CO^+ ion, a dipole induced in the orbiting ion shifts the measured cyclotron frequency. We use this cyclotron frequency shift to measure non-destructively the quantum state of the CO^+ ion. The effect also provides a means to determine to a few per cent the body-frame dipole moment of CO^+, thus establishing a method for measuring dipole moments of molecular ions for which few comparably accurate measurements exist[4–6]. The general perturbation that we describe here affects the most precise mass comparisons attainable today[7,8], with applications including direct tests of Einstein's mass–energy relationship[9] and charge-parity-time reversal symmetry[10], and possibly the weighing of chemical bonds[7].

The cyclotron frequency shift reported here for an ion with electric polarizability α can be understood using the exaggerated microscopic picture shown in Fig. 1. As the molecule (with net charge indicated by $+$) moves on its cyclotron orbit (solid circle) with velocity $\mathbf{v}$ perpendicular to the magnetic field $\mathbf{B}$, the Lorentz force is experienced in its instantaneous rest frame as a motional electric field $\mathbf{E}_m = \mathbf{v} \times \mathbf{B}$. The motional electric field induces a dipole $\mathbf{d}_{ind} = \alpha \mathbf{E}_m$ (modelled here by the outer $+$ and $-$ charges), which points towards the centre of the cyclotron orbit. As the ion orbits, the orientation of the induced dipole adiabatically follows the motional electric field (as indicated by the two snapshots at times t and $t + \Delta t$). As a result, the two ends of the induced dipole move at slightly different speeds (as emphasized by the dashed lines). The differential velocity gives rise to a net additional Lorentz force on the particle that is also directed along the radial direction. The size of the induced dipole is proportional to the ion's velocity, which for the circular cyclotron motion is proportional to its cyclotron radius. A constant frequency shift then results because the size of the additional Lorentz force scales linearly with the cyclotron radius, just as the original Lorentz force does. Equivalently, the cyclotron frequency shift occurs because the induced dipole moves the centre of charge to a radius different from that of the centre of mass. The fractional frequency shift is then simply given by the ratio of the distance between the two centres and the cyclotron radius.

This polarization force also occurs for neutral particles, and can be generally modelled as a renormalization of the inertial mass of the particle in the plane perpendicular to the magnetic field. If a neutral particle accelerates, the induced dipole relaxes to a new equilibrium value, creating a transient Lorentz force that either opposes or enhances the change in velocity, acting like a changed inertial mass. The new effective mass is given simply by $m_\lambda = m(1 + \alpha_\lambda B^2/m)$ where m is the usual inertial mass, and α_λ is the electric polarizability of the particle. This expression for the effective mass can be derived by including a phenomenological polarization

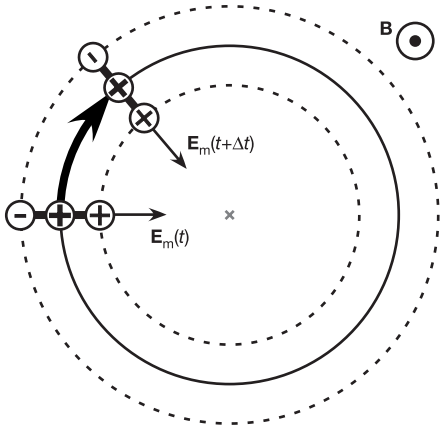

Figure 1 An exaggerated microscopic picture of the polarization force shift of the cyclotron frequency. As the molecule (with net charge indicated by $+$) moves on its cyclotron orbit (solid circle) perpendicular to the magnetic field $\mathbf{B}$, the magnetic field is experienced in its instantaneous rest frame as a motional electric field $\mathbf{E}_m$. The motional electric field induces a dipole (modelled here by the outer $+$ and $-$ charges), which points towards the centre of the cyclotron orbit. As the ion orbits, the orientation of the induced dipole adiabatically follows the motional electric field (as indicated by the two snapshots at times t and $t + \Delta t$). As a result, the two ends of the induced dipole move at slightly different speeds (as emphasized by the dashed lines) thus generating an additional Lorentz force. The orbital frequency then has to adjust in order to compensate for the additional force.